

Probing Quantum Criticality and Symmetry Breaking at the Microscopic Level

Vasily Makhlov, Tanish Satoor, Alexandre Evrard, Thomas Chalopin, Raphael Lopes, and Sylvain Nascimbene*
*Laboratoire Kastler Brossel, Collège de France, CNRS, ENS-PSL University, Sorbonne Université,
 11 Place Marcelin Berthelot, 75005 Paris, France*

 (Received 9 May 2019; published 18 September 2019)

We report on an experimental study of the Lipkin-Meshkov-Glick model of quantum spins interacting at infinite range in a transverse magnetic field, which exhibits a ferromagnetic phase transition in the thermodynamic limit. We use dysprosium atoms of electronic spin $J = 8$, subjected to a quadratic Zeeman light shift, to simulate $2J = 16$ interacting spins $1/2$. We probe the system microscopically using single magnetic sublevel resolution, giving access to the spin projection parity, which is the collective observable characterizing the underlying \mathbb{Z}_2 symmetry. We measure the thermodynamic properties and dynamical response of the system, and we study the quantum critical behavior around the transition point. In the ferromagnetic phase, we achieve coherent tunneling between symmetry-broken states, and we test the link between symmetry breaking and the appearance of a finite order parameter.

DOI: 10.1103/PhysRevLett.123.120601

From complex quantum materials such as cuprate superconductors to simple spin models, many-body systems close to a quantum critical point exhibit distinct properties driven by quantum fluctuations [1]. Some features, such as the slowing down of relaxation times, can be probed via macroscopic observables. However, revealing specifically quantum properties (e.g., many-body quantum entanglement [2]) remains challenging. The recent development of highly controlled quantum systems of mesoscopic size (such as ion crystals [3], ultracold gases [4], Rydberg atom arrays [5], or interacting photons [6]) allows for a microscopic characterization of collective quantum properties [7], e.g., the full density matrix [6], entanglement entropy [8], or nonlocal string order [9]. This degree of control could be used to investigate fundamental aspects of quantum phase transitions, such as the link between the breaking of an underlying symmetry and the onset of a nonzero-order parameter [10]. This connection cannot be tested in macroscopic systems because superselection rules forbid large-size quantum superpositions [11], making spontaneous symmetry breaking unavoidable [12].

In this Letter, we experimentally characterize at the microscopic level the Lipkin-Meshkov-Glick model (LMGM) consisting of N quantum spins with infinite-range Ising interactions in a transverse field. This model is applicable to nuclear systems [13,14], large-spin molecules [15], trapped ions [16,17], and two-mode [18–20] or spinor [21] Bose-Einstein condensates. Our study is based on the equivalence between the electronic spin $J = 8$ of dysprosium atoms and a set of $N = 16$ spins $1/2$ symmetric upon exchange [22], with Ising interactions simulated via a light-induced quadratic Zeeman shift [23]. In the thermodynamic limit (TL), the LMGM exhibits a ferromagnetic phase transition (see Fig. 1) characterized by spontaneous

breaking of a \mathbb{Z}_2 symmetry—the parity of the total z spin projection. We measure a crossover between paramagnetic and ferromagnetic behaviors, which are separated by a quantum critical regime where we observe nonclassical behavior and a minimum of the energy gap [24,25]. A specific asset of our setup is the direct access to the quantum state parity, which is a collective observable

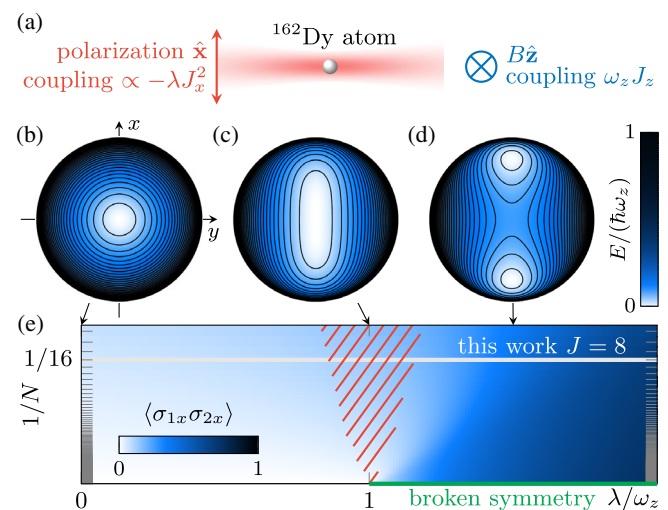


FIG. 1. (a) Scheme of experiment, based on laser-induced dynamics of the electronic spin of dysprosium atoms (quadratic light shift of $\propto -\lambda J_x^2$) in the presence of a magnetic field (Zeeman coupling $\omega_z J_z$). (b), (c), and (d) Classical energy landscapes on the southern hemisphere of the generalized Bloch sphere for $\lambda = 0$, ω_z , and $1.5\omega_z$, respectively. (e) Finite-size phase diagram, showing the spin pair correlator $\langle \sigma_{1x} \sigma_{2x} \rangle$, with a ferromagnetic phase in the thermodynamic limit for $\lambda > \omega_z$ (green line). For a finite N , the phase transition is smoothed over a quantum critical region (dashed red area).

hidden in macroscopic systems such as large ensembles of spins $1/2$. We show that the \mathbb{Z}_2 symmetry breaking is directly related to the onset of a nonzero-order parameter.

The LMGM is described by the Hamiltonian

$$H = -\frac{\hbar\lambda}{4(N-1)} \sum_{1 \leq i \neq j \leq N} \sigma_{ix} \sigma_{jx} + \frac{\hbar\omega_z}{2} \sum_{1 \leq i \leq N} \sigma_{iz}. \quad (1)$$

Here, $\hbar\sigma_{iu}/2$ denotes the projection of the spin i along u ($1 \leq i \leq N$), the factor $1/(N-1)$ ensures extensivity of the energy for large N [26], and we restrict ourselves to ferromagnetic interactions of $\lambda > 0$. Although the exact ground state is not a product state [27], thermodynamic quantities are well described by the classical mean-field theory in the TL because each spin interacts with the sum of all other spins [24]. The corresponding classical energy functionals, parametrized by the mean spin orientation, are shown in Figs. 1(b)–1(d) for $\lambda = 0$, ω_z , and $1.5\omega_z$. They reveal the occurrence of a quantum phase transition between a paramagnetic phase for $\lambda < \omega_z$ and a ferromagnetic phase for $\lambda > \omega_z$, for which the system exhibits two degenerate ground states with nonzero-order parameter $\langle \sigma_{1x} \rangle \neq 0$. Furthermore, the \mathbb{Z}_2 symmetry, associated to the conservation of parity,

$$P_z = \prod_{i=1}^N \sigma_{i,z},$$

is spontaneously broken at the transition point. Introducing the collective spin

$$\mathbf{J} = \frac{1}{2} \sum_i \boldsymbol{\sigma}_i,$$

the Hamiltonian [Eq. (1)] can be recast (up to an overall energy shift) as

$$H = -\frac{\hbar\lambda}{2J-1} J_x^2 + \hbar\omega_z J_z. \quad (2)$$

For ferromagnetic interactions, its lowest-energy states are permutationally symmetric and their collective spin has the maximal length of $J = N/2$.

In this work, we study the nonlinear dynamics of the electronic spin of $J = 8$ of ^{162}Dy atoms, simulating a ferromagnetic LMGM with $N = 16$ spins $1/2$. We use ultracold samples of $1.3(3) \times 10^5$ atoms, which are initially held in an optical dipole trap at a temperature of $T \simeq 1.1(1) \mu\text{K}$. The atomic spin is initially polarized in the ground state $| -J \rangle_z$, under a magnetic field $\mathbf{B} = B\hat{\mathbf{z}}$ with $B = 114(1) \text{ mG}$, corresponding to a Larmor frequency of $\omega_z = 2\pi \times 198(2) \text{ kHz}$. In this state, the N elementary spins are antialigned with the magnetic field, corresponding to a paramagnetic state. We then switch off the trap before applying a laser beam close to the 626 nm

optical transition, coupling the spin J to an excited electronic state of spin $J' = 9$. Given the transition line-width of $\Gamma \simeq 0.86 \mu\text{s}^{-1}$ and the detuning from resonance of $\simeq 20 \text{ GHz}$, we expect negligible incoherent Rayleigh scattering on the timescale of the experiment. The light is linearly polarized along x , producing a quadratic Zeeman shift proportional to J_x^2 [23], up to a spin-independent energy shift that does not influence the spin dynamics. The laser beam waist of $w = 50 \mu\text{m}$ is large enough to ensure uniform intensity over the atomic sample (rms size of $\sigma \simeq 5 \mu\text{m}$). For the maximum available light power ($P \simeq 1 \text{ W}$), we reach a ferromagnetic coupling of $\lambda \simeq 4\omega_z$ deep in the ferromagnetic phase. In the following, the coupling λ is adjusted via the light intensity on the atoms. After a typical evolution time of $t \sim 100 \mu\text{s}$, we switch off the light beam and apply time-dependent magnetic fields to perform arbitrary spin rotations before making a projection measurement along z . Combining rotation and projection gives us access to the spin projection probabilities of $\Pi_m(\hat{\mathbf{n}})$ ($-J \leq m \leq J$) along any direction $\hat{\mathbf{n}}$ [28].

We first investigate the properties of the ground state of the LMGM. We start with all atoms in the state $| -J \rangle_z$, which is the (paramagnetic) ground state for $\lambda = 0$. We then slowly ramp the light coupling from zero up to a final value λ using a linear ramp of speed $\dot{\lambda} \simeq 0.015\omega_z^2$, for which we expect quasiadiabatic evolution [29]. The measured spin projection probabilities $\Pi_m(\hat{\mathbf{n}})$ ($\hat{\mathbf{n}} = \hat{\mathbf{x}}, \hat{\mathbf{y}}, \hat{\mathbf{z}}$) are shown in Figs. 2(a), 2(c), and 2(e). We first consider the occurrence of a ferromagnetic ground state by measuring the order parameter $\langle \sigma_{1x} \rangle$. We show in Fig. 2(a) the single-shot projections $\Pi_m(\hat{\mathbf{x}})$ measured for various couplings λ . For small λ , we find a single-peak distribution centered on zero, which is consistent with the state $| -J \rangle_z$ projected along $\hat{\mathbf{x}}$. For $\lambda \gtrsim \omega_z$, we observe a bifurcation towards a double-peak distribution, which is consistent with population of the two broken-symmetry states: each with an order parameter of $\langle \sigma_{1x} \rangle \neq 0$. As the distributions remain globally symmetric, the system does not seem to choose a single broken state. With our measurement being averaged over many atoms, we cannot exclude a situation with almost half of the atoms in each broken state, e.g., organized in unresolved spin domains. This scenario is invalidated by a direct measurement of the mean parity $p_z \equiv \langle P_z \rangle$ that remains close to unity for all interaction strengths [see Fig. 2(f)]. Such an absence of symmetry breaking is, in fact, expected for a finite-size system, for which the ground state remains nondegenerate, as will be discussed later. The ground state prepared in the ferromagnetic phase exhibits both a large-spin projection variance along x and a well-defined parity along z , which is characteristic of a mesoscopic quantum superposition that is useful for quantum-enhanced metrology [33,34].

We now characterize the thermodynamic properties that are independent of the symmetry breaking itself. We probe ferromagnetic spin correlations, i.e., the relative alignment

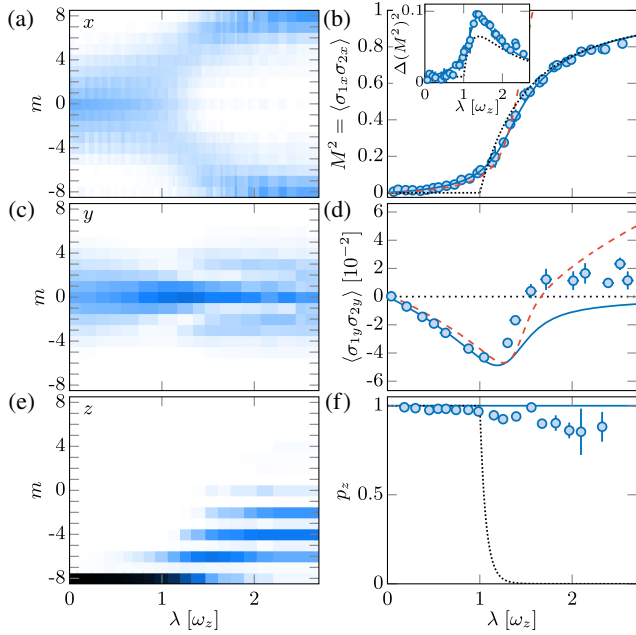


FIG. 2. (a), (c), and (e) Measured projection probabilities $\Pi_m(\hat{\mathbf{n}})$ for $\hat{\mathbf{n}} = \hat{\mathbf{x}}, \hat{\mathbf{y}},$ and $\hat{\mathbf{z}}$ [Figs. 2(a), 2(c), and 2(e), respectively] as a function of the interaction strength λ . (b), (d), and (f) Evolution of the spin pair correlator $\langle \sigma_{1x}\sigma_{2x} \rangle$ [Fig. 2(b)], its variance [inset of Fig. 2(b)], the correlator $\langle \sigma_{1y}\sigma_{2y} \rangle$ [Fig. 2(d)], and the mean parity p_z [Fig. 2(f)]. Solid blue, dotted black, and dashed red lines correspond to the LMGM, the classical mean-field model, and the critical Hamiltonian, respectively. No averaging is performed in Fig. 2(a). In other panels, all data are the averages of about five independent measurements. In all figures, error bars represent the $1\text{-}\sigma$ statistical uncertainty.

between spins along $\hat{\mathbf{x}}$ quantified by the correlator $M^2 \equiv \langle \sigma_{1x}\sigma_{2x} \rangle$ [24]. We compute it from the second moment of the measured probabilities $\Pi_m(\hat{\mathbf{x}})$ using $N+N(N-1)$ $\langle \sigma_{1\hat{\mathbf{n}}}\sigma_{2\hat{\mathbf{n}}} \rangle = 4\langle J_{\hat{\mathbf{n}}}^2 \rangle$ [35]. As shown in Fig. 2(b), we measure a smooth increase of M^2 as a function of λ , which is consistent with a crossover between paramagnetic and ferromagnetic behaviors. We compare our measurements with various theoretical models: namely, the $N = 16$ LMGM (blue lines in Fig. 2), the mean-field model corresponding to the $N \rightarrow \infty$ limit (dotted black lines), and its first finite- N correction close to the critical point, as will be discussed below (dashed red lines). As shown in Fig. 2(b), the measured ferromagnetic correlator M^2 agrees with the $N = 16$ LMGM for all couplings λ , and it remains close to the mean-field theory for most values of λ , except around $\lambda = \omega_z$ [29,36]. In the critical regime, the leading $1/N$ finite-size correction can be simply formulated because the quantum ground state remains close to the coherent state $|-J\rangle_z$ such that operators J_x and J_y are almost canonically conjugated variables with $[J_x, J_y] = iJ_z \simeq -iJ$ [37]. This approximation leads to a low-energy “critical” Hamiltonian [29,38,39]

$$\frac{H_c}{\hbar\omega_z} = -\left(J + \frac{1}{2}\right) + \frac{1}{J^{1/3}} \left(\frac{P^2}{2} - \frac{\epsilon X^2}{2} + \frac{X^4}{8} \right), \quad (3)$$

describing the dynamics of a massive particle in a harmonic plus quartic potential, where $\epsilon = J^{2/3}(\lambda/\omega_z - 1)$, $X = J^{-2/3}J_x$, and $P = -J^{-1/3}J_y$. This description matches the textbook Landau picture of a second-order phase transition evolving from single- to double-well potentials when crossing the critical point at $\epsilon = 0$ [10]. As plotted in Fig. 2(b), the universal Hamiltonian [Eq. (3)] is sufficient to account for the measured deviations to the TL well around $\lambda = \omega_z$ [40].

We also investigated signatures of the phase transition itself in our finite-size system. First, we measured an increase of fluctuations of the ferromagnetic correlator $\Delta(M^2) \equiv \Delta(J_x^2)/[J(J - \frac{1}{2})]^2$ around the critical point of $\lambda = \omega_z$ [see inset of Fig. 2(b)]—a generic feature of continuous phase transitions [41]. More specifically, quantum phase transitions are also associated with the onset of entanglement in the critical region [1]. *A priori*, probing quantum entanglement requires partitioning the electronic spin J , which is forbidden at low energy but could, in principle, be achieved using coherent optical transitions $J \rightarrow J'$ [42,43]. Yet, we can indirectly probe entanglement in our system via spin projection correlations. Indeed, separable states that are symmetric upon exchange satisfy $\langle \sigma_{1\hat{\mathbf{n}}}\sigma_{2\hat{\mathbf{n}}} \rangle = \langle \sigma_{1\hat{\mathbf{n}}} \rangle^2$ for all projection directions $\hat{\mathbf{n}}$, and thus can only exhibit positive correlators [35,44]. As shown in Figs. 2(c) and 2(d), we measure the correlator $\langle \sigma_{1y}\sigma_{2y} \rangle$ and show that it assumes negative values in a broad range of interaction strengths [45], which is consistent with entanglement and suggests that the phase transition is driven by quantum (rather than thermal) fluctuations [2,47]. The measured correlator—including its minimum value—is consistent with the LMGM prediction for $\lambda < \omega_z$. In the ferromagnetic phase, the measured correlator significantly exceeds the expected values, which we attribute to shot-to-shot variations of the spin rotation parameters used for the y spin projection due to magnetic field fluctuations.

We now extend our study to the system dynamics by measuring the energy gap of low-lying excitations. Due to the \mathbb{Z}_2 symmetry of the LMGM, the eigenstates can be divided into two sectors of even and odd parities. The low-energy dynamics is then governed by two energy gaps, namely, the “parity” gap $\hbar\delta$ between opposite-parity ground states and the “dynamical” gap $\hbar\Delta$ between the lowest two energy levels of even parity. In the effective potential picture, these gaps correspond to the oscillation frequencies of the dipole (δ) and breathing (Δ) modes. To excite the breathing mode, we simply increase the ramp speed $\dot{\lambda}$ used for the state preparation, leading to a diabatic population of the first excited state of even parity while keeping the higher states almost unpopulated. We then measure the time evolution of the second moment $\langle \sigma_{1x}\sigma_{2x} \rangle$,

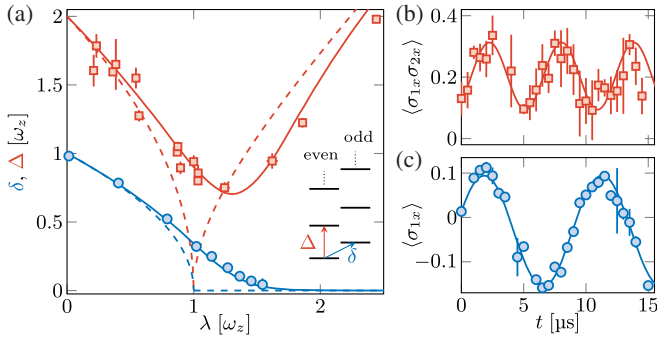


FIG. 3. (a) Parity gap δ between even- and odd-parity sectors, and dynamical gap Δ between the ground and first even-parity states as a function of the coupling λ . Solid (dashed) lines are LMG (mean-field) predictions. [(a) inset] Energy level scheme of the six lowest eigenstates for $\lambda = 0.5\omega_z$. (b) Breathing mode oscillation performed for $\lambda = 1.04(2)\omega_z$. The solid line is a sine fit of frequency Δ . (c) Dipole mode oscillation performed for $\lambda = 0.79(2)\omega_z$. The solid line is a sine fit of frequency δ .

and we extract its oscillation frequency Δ [see Fig. 3(b)]. To excite the dipole mode, we first prepare the ground state for a given coupling λ , and we apply a parity-breaking perturbation using a pulse of the magnetic field along x of duration $t \simeq 3 \mu\text{s}$, coupling the ground state to the odd-parity sector. The amplitude is chosen small enough to only populate the even- and odd-parity ground states, and the first moment's $\langle \sigma_{1x} \rangle$ oscillation frequency (δ) is extracted [see Fig. 3(c)].

The measured parity and dynamical gaps, reported in Fig. 3(a), agree well with the LMG. The dynamical gap Δ exhibits a minimum around the critical point, which is reminiscent of the closing of the gap in the TL at the transition point. The parity gap δ decreases when increasing the coupling λ , which is in analogy with the softening of the spin dipole mode in quantum systems close to a ferromagnetic transition [48,49]. In the paramagnetic phase of $\lambda \lesssim 0.5\omega_z$, the dynamical gap Δ remains about twice the parity gap δ , which is consistent with a picture of non-interacting excitation quanta [25,37]. At the critical point, the measured dynamical gap of $\Delta = 0.91(5)\omega_z$ significantly exceeds twice the parity gap of $\delta = 0.33(1)\omega_z$, which is as expected from particle dynamics in a quartic potential [see Eq. (3) for $\epsilon = 0$]. This nonharmonic behavior illustrates the generic behavior of quantum critical systems, for which the low-energy spectra cannot be simply reduced to noninteracting excitation quanta [1]. The gap value for $\lambda = \omega_z$ is also consistent with the leading finite-size correction to the mean field $\Delta/\omega_z \simeq 1.78/J^{1/3} = 0.89$, which is valid for $J \gg 1$ [24,50,51].

We now focus on the dipole oscillation measurements in the ferromagnetic phase, where we measure a strong reduction of the parity gap [see Fig. 4(a)]. The even- and odd-parity ground states thus become almost degenerate, which is a behavior reminiscent of the exact double degeneracy expected in the TL for $\lambda > \omega_z$. We show, in

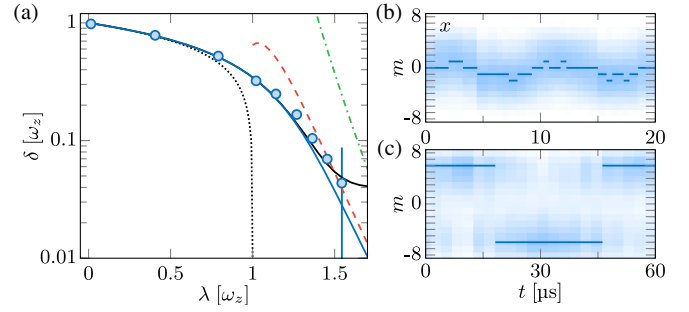


FIG. 4. (a) Parity gap δ as a function of λ (blue dots) compared with LMG (blue line), mean-field theory (black dotted line), semiclassical tunneling (red dashed line), and perturbation theories (green dash-dotted line). The solid black line is the mean value of δ expected from the LMG and averaged over magnetic field fluctuations. (b) and (c) Time evolutions of projection probabilities $\Pi_m(\hat{\mathbf{x}})$ during dipole mode oscillation for $\lambda = 0.79(2)\omega_z$ [Fig. 4(b)] and $\lambda = 1.36(2)\omega_z$ [Fig. 4(c)]. The most probable projection m^* is plotted as a blue line.

Figs. 4(b) and 4(c), the time evolutions of the probability distributions $\Pi_m(\hat{\mathbf{x}})$ during the dipole oscillation in the paramagnetic [Fig. 4(b)] and ferromagnetic [Fig. 4(c)] phases. In the paramagnetic phase, the distributions always exhibit a single peak for which the center smoothly oscillates around zero. On the contrary, in the ferromagnetic phase, the distributions exhibit two peaks at positive or negative large- $|m|$ values, and the dynamics consists of an oscillation between the peak weights, without significantly populating small- $|m|$ states. This qualitatively different behavior is well illustrated by the evolution of the most probable projection m^* , which only takes two possible values of $m^* = \pm 6$ during the evolution shown in Fig. 4(c). These maximal projection values are close to the collective spin projections of $\langle J_x \rangle = \pm 5.4(5)$ of the two mean-field broken-symmetry states for $\lambda = 1.36(2)\omega_z$. Such a dynamics can be interpreted as a “macroscopic” quantum tunneling regime between broken states—a phenomenon studied extensively in large-spin molecules [15,52–54] and

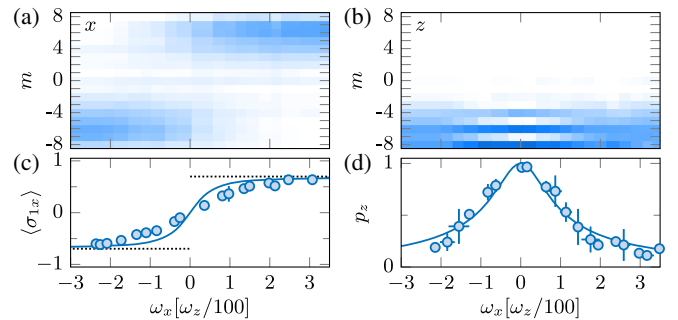


FIG. 5. (a) and (b) Projection probabilities $\Pi_m(\hat{\mathbf{x}})$ [Fig. 5(a)] and $\Pi_m(\hat{\mathbf{z}})$ [Fig. 5(b)] in the ground state as a function of ω_x for $\lambda = 1.40(3)\omega_z$. (c) and (d) Order parameter $\langle \sigma_{1x} \rangle$ and mean parity p_z computed from Figs. 5(a) and 5(b) and compared to the LMG (solid lines) and the mean-field order parameter values (dotted lines).

superconducting quantum interference device systems [55–57]. Deep in the ferromagnetic phase, the dipole frequencies are consistent with the semiclassical theory of quantum tunneling [58–60]. In the limit $\lambda \gg \omega_z$, the perturbation theory provides a simple picture of this behavior: the two broken states $|\pm J\rangle_x$ being coupled by the z field via a $2J$ -order process leads to a high power-law scaling of $\delta/\omega_z \propto (\omega_z/\lambda)^{2J-1}$. For values of $\lambda \gtrsim 1.5\omega_z$, the oscillation contrast decreases and the measured frequency deviates from theory, which we attribute to residual magnetic field fluctuations along x (rms width of $\sigma_B = 0.4$ mG), inducing an offset between the two wells that exceeds the tunnel coupling.

We finally investigate the controlled breaking of parity symmetry by a static magnetic field applied along x , which adds a Zeeman coupling of $-\hbar\omega_x J_x$ mixing the two parity sectors. As shown in Fig. 4, this field simultaneously induces a finite order parameter $\langle\sigma_{1x}\rangle$ and a reduction of the mean parity p_z . For large fields, the order parameter reaches a plateau consistent with the mean-field prediction of $\langle\sigma_{1x}\rangle = \text{sgn}(\omega_x)\sqrt{1 - (\omega_z/\lambda)^2}$. This behavior coincides with a cancellation of the mean parity p_z , illustrating the link between broken-symmetry and nonzero order parameter [29]. Besides the controlled symmetry breaking discussed above, spontaneous symmetry breaking also occurs in our system when preparing the ground state in the ferromagnetic phase using very slow ramps of the light coupling of $\dot{\lambda} \simeq 10^{-3}\omega_z^2$. We find that the sign of the spontaneous order parameter $\langle\sigma_{1x}\rangle$ is directly related to the sign of the shot-to-shot magnetic field fluctuation, which is independently recorded. We found no signature of more complex symmetry-breaking mechanisms, e.g., induced by interactions between atoms [61].

In conclusion, we studied the ground state and low-energy spectrum of the LMGM via nonlinear dynamics of the electronic spin of ^{162}Dy atoms. A possible extension of this study would be the nonadiabatic crossing of the critical point, which is a problem related to quantum annealing [62] and the Kibble-Zurek mechanism—for which the relevance for infinitely coordinated systems is debated [63–67]. In the ferromagnetic phase, we have demonstrated the production of the coherent superposition of broken-symmetry states [68] of interest for quantum-enhanced metrology [69]. Our system is also well suited to investigate various spontaneous symmetry-breaking mechanisms at the microscopic level and their connection to decoherence [70,71]. Our work could also be generalized to systems with an internal spin of larger amplitude, such as large-spin molecules [15,72] or Rydberg atoms [73].

We thank J. Dalibard, L. Glazman, and P. Ribeiro for stimulating discussions, as well as J. Beugnon, J. Dalibard, and F. Gerbier for a careful reading of the Letter. This work is supported by PSL University (MAFAG project) and the European Union (ERC UQUAM and TOPODY).

V. M. and T. S. contributed equally to this work.

*sylvain.nascimbene@lkb.ens.fr

- [1] S. Sachdev, *Quantum Phase Transitions* (Cambridge University Press, Cambridge, England, 2011).
- [2] A. Osterloh, L. Amico, G. Falci, and R. Fazio, *Nature (London)* **416**, 608 (2002).
- [3] R. Blatt and C. F. Roos, *Nat. Phys.* **8**, 277 (2012).
- [4] C. Gross and I. Bloch, *Science* **357**, 995 (2017).
- [5] M. Saffman, *J. Phys. B* **49**, 202001 (2016).
- [6] X.-s. Ma, B. Dakic, W. Naylor, A. Zeilinger, and P. Walther, *Nat. Phys.* **7**, 399 (2011).
- [7] I. M. Geogescu, S. Ashhab, and F. Nori, *Rev. Mod. Phys.* **86**, 153 (2014).
- [8] R. Islam, R. Ma, P. M. Preiss, M. Eric Tai, A. Lukin, M. Rispoli, and M. Greiner, *Nature (London)* **528**, 77 (2015).
- [9] T. A. Hilker, G. Salomon, F. Grusdt, A. Omran, M. Boll, E. Demler, I. Bloch, and C. Gross, *Science* **357**, 484 (2017).
- [10] L. D. Landau, *Ukr. J. Phys.* **11**, 19 (1937).
- [11] S. D. Bartlett, T. Rudolph, and R. W. Spekkens, *Rev. Mod. Phys.* **79**, 555 (2007).
- [12] P. Anderson, *Basic Notions of Condensed Matter Physics* (Benjamin Cummings, San Francisco, 1984).
- [13] H. J. Lipkin, N. Meshkov, and A. J. Glick, *Nucl. Phys.* **62**, 188 (1965).
- [14] P. Cejnar, J. Jolie, and R. F. Casten, *Rev. Mod. Phys.* **82**, 2155 (2010).
- [15] D. Gatteschi and R. Sessoli, *Angew. Chem., Int. Ed.* **42**, 268 (2003).
- [16] B. P. Lanyon, C. Hempel, D. Nigg, M. Müller, R. Gerritsma, F. Zähringer, P. Schindler, J. T. Barreiro, M. Rambach, G. Kirchmair, M. Hennrich, P. Zoller, R. Blatt, and C. F. Roos, *Science* **334**, 57 (2011).
- [17] R. Islam, E. E. Edwards, K. Kim, S. Korenblit, C. Noh, H. Carmichael, G.-D. Lin, L.-M. Duan, C.-C. Joseph Wang, J. K. Freericks, and C. Monroe, *Nat. Commun.* **2**, 377 (2011).
- [18] M. Albiez, R. Gati, J. Fölling, S. Hunsmann, M. Cristiani, and M. K. Oberthaler, *Phys. Rev. Lett.* **95**, 010402 (2005).
- [19] S. Levy, E. Lahoud, I. Shomroni, and J. Steinhauer, *Nature (London)* **449**, 579 (2007).
- [20] A. Trenkwalder, G. Spagnolli, G. Semeghini, S. Coop, M. Landini, P. Castilho, L. Pezzè, G. Modugno, M. Inguscio, A. Smerzi, and M. Fattori, *Nat. Phys.* **12**, 826 (2016).
- [21] T. Zibold, E. Nicklas, C. Gross, and M. K. Oberthaler, *Phys. Rev. Lett.* **105**, 204101 (2010).
- [22] L. D. Landau and E. Lifshitz, *Quantum Mechanics, Non-Relativistic Theory* (Pergamon, London, 1958).
- [23] G. A. Smith, S. Chaudhury, A. Silberfarb, I. H. Deutsch, and P. S. Jessen, *Phys. Rev. Lett.* **93**, 163602 (2004).
- [24] R. Botet, R. Jullien, and P. Pfeuty, *Phys. Rev. Lett.* **49**, 478 (1982).
- [25] S. Dusuel and J. Vidal, *Phys. Rev. Lett.* **93**, 237204 (2004).
- [26] A. Campa, T. Dauxois, D. Fanelli, and S. Ruffo, *Physics of Long-Range Interacting Systems* (Oxford University, New York, 2014).
- [27] R. Orús, S. Dusuel, and J. Vidal, *Phys. Rev. Lett.* **101**, 025701 (2008).
- [28] A. Evrard, V. Makhlov, T. Chalopin, L. A. Sidorenkov, J. Dalibard, R. Lopes, and S. Nascimbene, *Phys. Rev. Lett.* **122**, 173601 (2019).
- [29] See Supplemental Material at <http://link.aps.org/supplemental/10.1103/PhysRevLett.123.120601> for a study

- of adiabaticity requirements for the ground state preparation, eigenstate spectroscopy at higher energy, a description of the classical mean-field treatment, a derivation of the critical Hamiltonian, and an extensive discussion of parity symmetry breaking by an external magnetic field. It includes Refs. [30–32].
- [30] F. T. Hioe, D. MacMillen, and E. W. Montroll, *Phys. Rep.* **43**, 305 (1978).
- [31] F. Leyvraz and W. D. Heiss, *Phys. Rev. Lett.* **95**, 050402 (2005).
- [32] M. Heyl, *Rep. Prog. Phys.* **81**, 054001 (2018).
- [33] J. J. Bollinger, W. M. Itano, D. J. Wineland, and D. J. Heinzen, *Phys. Rev. A* **54**, R4649 (1996).
- [34] C. Lee, *Phys. Rev. Lett.* **97**, 150402 (2006).
- [35] D. Ulam-Orgikh and M. Kitagawa, *Phys. Rev. A* **64**, 052106 (2001).
- [36] L. Landau, L. Pitaevskii, and E. Lifshitz, *Electrodynamics of Continuous Media* (Butterworth, Washington, DC, 1984).
- [37] T. Holstein and H. Primakoff, *Phys. Rev.* **58**, 1098 (1940).
- [38] V. V. Ulyanov and O. B. Zaslavskii, *Phys. Rep.* **216**, 179 (1992).
- [39] The Hamiltonian [Eq. (3)] corresponds to a $1/N$ expansion of the LMGM at fixed ϵ , which is expected to be valid in the range $\lambda/\omega_z - 1 \lesssim 1/4$ [29].
- [40] It becomes inaccurate in the deep ferromagnetic phase (for $\lambda \gtrsim 1.5\omega_z$, see [29]), where the precise shape of the double-well potential is required to describe quantitatively the quantum tunneling effects [38].
- [41] L. Landau and E. Lifshitz, in *Statistical Physics* (Butterworth-Heinemann, Oxford, England, 1980), 3rd ed., pp. 446–516.
- [42] O. Gühne and G. Tóth, *Phys. Rep.* **474**, 1 (2009).
- [43] N. Killoran, M. Cramer, and M. B. Plenio, *Phys. Rev. Lett.* **112**, 150501 (2014).
- [44] J. Vidal, *Phys. Rev. A* **73**, 062318 (2006).
- [45] The minimum value $\langle \sigma_{1y}\sigma_{2y} \rangle = -0.040(5)$ for $\lambda \simeq \omega_z$ is about 60% of the minimum correlation $\langle \sigma_{1\hat{n}}\sigma_{2\hat{n}} \rangle = -1/(N-1)$ allowed for a set of N spins that are symmetric upon exchange [46].
- [46] M. Koashi, V. Bužek, and N. Imoto, *Phys. Rev. A* **62**, 050302(R) (2000).
- [47] X.-Y. Luo, Y.-Q. Zou, L.-N. Wu, Q. Liu, M.-F. Han, M. K. Tey, and L. You, *Science* **355**, 620 (2017).
- [48] A. Sartori, J. Marino, S. Stringari, and A. Recati, *New J. Phys.* **17**, 093036 (2015).
- [49] G. Valtolina, F. Scazza, A. Amico, A. Burchianti, A. Recati, T. Enss, M. Inguscio, M. Zaccanti, and G. Roati, *Nat. Phys.* **13**, 704 (2017).
- [50] S. Dusuel and J. Vidal, *Phys. Rev. B* **71**, 224420 (2005).
- [51] We present in the Supplemental Material [29] measurements of higher-energy levels that confirm this picture on a larger energy range.
- [52] S. A. Owerre and M. B. Paranjape, *Phys. Rep.* **546**, 1 (2015).
- [53] J. R. Friedman, M. P. Sarachik, J. Tejada, and R. Ziolo, *Phys. Rev. Lett.* **76**, 3830 (1996).
- [54] L. Thomas, F. Lioni, R. Ballou, D. Gatteschi, R. Sessoli, and B. Barbara, *Nature (London)* **383**, 145 (1996).
- [55] J. R. Friedman, V. Patel, W. Chen, S. K. Tolpygo, and J. E. Lukens, *Nature (London)* **406**, 43 (2000).
- [56] C. H. van der Wal, A. C. J. ter Haar, F. K. Wilhelm, R. N. Schouten, C. J. P. M. Harmans, T. P. Orlando, S. Lloyd, and J. E. Mooij, *Science* **290**, 773 (2000).
- [57] Y. Makhlin, G. Schön, and A. Shnirman, *Rev. Mod. Phys.* **73**, 357 (2001).
- [58] M.ENZ and R. Schilling, *J. Phys. C* **19**, 1765 (1986).
- [59] G. Scharf, W. F. Wreszinski, van, and J. L. Hemmen, *J. Phys. A* **20**, 4309 (1987).
- [60] O. B. Zaslavskii, *Phys. Lett. A* **145**, 471 (1990).
- [61] We did not observe a significant reduction of parity when increasing the atomic density (up to $\sim 10^{14}$ cm $^{-3}$).
- [62] V. Bapst and G. Semerjian, *J. Stat. Mech.* (2012) P06007.
- [63] T. Caneva, R. Fazio, and G. E. Santoro, *Phys. Rev. B* **78**, 104426 (2008).
- [64] P. Solinas, P. Ribeiro, and R. Mosseri, *Phys. Rev. A* **78**, 052329 (2008).
- [65] O. L. Acevedo, L. Quiroga, F. J. Rodríguez, and N. F. Johnson, *Phys. Rev. Lett.* **112**, 030403 (2014).
- [66] M.-J. Hwang, R. Puebla, and M. B. Plenio, *Phys. Rev. Lett.* **115**, 180404 (2015).
- [67] N. Defenu, T. Enss, M. Kastner, and G. Morigi, *Phys. Rev. Lett.* **121**, 240403 (2018).
- [68] J. I. Cirac, M. Lewenstein, K. Mølmer, and P. Zoller, *Phys. Rev. A* **57**, 1208 (1998).
- [69] L. Pezzè, A. Smerzi, M. K. Oberthaler, R. Schmied, and P. Treutlein, *Rev. Mod. Phys.* **90**, 035005 (2018).
- [70] M. Lucamarini, S. Paganelli, and S. Mancini, *Phys. Rev. A* **69**, 062308 (2004).
- [71] J. van Wezel, J. van den Brink, and J. Zaanen, *Phys. Rev. Lett.* **94**, 230401 (2005).
- [72] J. Floß, A. Kamalov, I. S. Averbukh, and P. H. Bucksbaum, *Phys. Rev. Lett.* **115**, 203002 (2015).
- [73] A. Facon, E.-K. Dietsche, D. Grosso, S. Haroche, J.-M. Raimond, M. Brune, and S. Gleyzes, *Nature (London)* **535**, 262 (2016).